Characterization of gas crossover and its implications in PEM fuel cells. AlChE J

3 AUTHORS, INCLUDING:

Shyam Kocha
National Renewable Energy Laboratory
58 PUBLICATIONS **3,082** CITATIONS

SEE PROFILE

Jung S. Yi
Pynus Cable
20 PUBLICATIONS **1,683** CITATIONS

SEE PROFILE

Characterization of Gas Crossover and Its Implications in PEM Fuel Cells

Shyam S. Kocha, J. Deliang Yang, and Jung S. Yi
UTC Fuel Cells, South Windsor, CT 06074

With pure hydrogen as the fuel, PEM fuel cell operation at or near 100% fuel utilization is desirable to achieve a high stack efficiency and zero emissions. However, typical membranes used in PEM fuel cells allow a finite amount of permeation rates or crossover of hydrogen, oxygen, and nitrogen across the membrane. The hydrogen and oxygen that permeate through the membrane are consumed with the generation of heat and water but without the generating of useful work, leading to a fuel inefficiency. Nitrogen crossover, on the other hand, from the cathode side to the anode side accumulates at the exit of the anode flow fields, lowering the hydrogen concentration and resulting in local fuel starvation. In this study, an in-situ electrochemical technique has been applied to determine the magnitude of the hydrogen crossover over a range of relevant fuel cell operating temperatures and pressures. Permeability coefficients thus obtained are compared to values reported in the literature. A mathematical model is developed to predict the extent of nitrogen accumulation along the anode flow fields, and fuel recycle as a mitigation method is simulated by improving hydrogen distribution. The model results were validated by comparison with experimental results.© 2006 American Institute of Chemical Engineers AIChE J, 52: 1916–1925, 2006
Keywords: PEM fuel cell, fuel efficiency, gas crossover, hydrogen, permeability

Introduction

The reasons for the current interest in hydrogen powered fuel cell engine development are well documented.[1] The advantages of proton exchange membrane (PEM) fuel cells include a high fuel efficiency and the potential for zero emissions. When hydrogen is used as the fuel with air as the oxidant, the only reaction product is pure water, although in practice unused hydrogen from the anode and unused oxygen and nitrogen from the cathode are also released to the atmosphere. The unused hydrogen has to be combusted in a catalytic exhaust burner or recirculated using an anode recycle pump to meet hydrogen emission safety standards.

Currently, perfluorosulfonic acid based membranes such as the Nafion® type of membrane are commonly employed as the electrolyte for PEM fuel cells. The membrane serves the purposes of: (1) a barrier between the anode and cathode reactants, (2) proton conduction, and (3) electronic insulator. This type of membrane performs effectively and exhibits high lifetimes only when it is well hydrated. Water is generated at the cathode side due to electrochemical reaction. It also migrates with the protons from the anode to the cathode by electro-osmosis. Consequently, membrane dehydration is often reported on the anode even though some back diffusion of water takes place from the cathode to the anode side due to buildup of a concentration gradient of water across the membrane. Significant effort has been directed toward minimizing membrane thickness to lower the ionic resistance of protons in the membrane and also to promote self-adjustment of water content by increasing the gradient between the anode and cathode sides of

the membrane. The target attributes of high proton conductivity and low areal resistance are provided by a high ion exchange capacity (low equivalent weight) and a thin film. These attributes have to be balanced with the conflicting requirements of high physical stability and low reactant permeation rate. In the attempt to balance these requirements, practical proton exchange membranes of reasonable thickness and equivalent weight allow a limited amount of crossover of reactants across the membrane.

A further requirement for the PEM used in the solubilized form at the fuel cell cathode is a high permeability to oxygen to lower the mass transfer resistance at the cathode. Fortunately, Nafion® like materials have a permeability that is suitable both for use as a membrane as well as solubilized ionomer in the electrodes.

The use of a thinner membrane has allowed us to achieve high power densities due to a lower ohmic loss in the membrane. The hydrogen and oxygen that permeate through the membrane are consumed with the generation of heat and water without the generating of useful work, leading to a fuel inefficiency. Since the hydrogen permeation rates are of the order of a few milliamp to tens of milliamp per squire centimeter while the oxygen permeates at about half the rate of hydrogen,[2] the voltage obtained at low current densities, below 0.1 A/cm^2, is significantly affected and especially so under high-pressure operations. This results in the apparent catalytic activity of Pt/C in Nafion measured from fuel cell configuration to be depressed, making it difficult to evaluate the catalytic activity of the catalyst at the electrode. The apparent activity losses due to crossover have to be corrected for proper estimation of the activity of the Pt catalyst. More importantly, oxygen permeation through the membrane can cause the formation of peroxide and hydroperoxide radicals in the membrane that can be a source of membrane degradation, reducing the life-span of PEM fuel cell stacks.[3] In addition, the inert nitrogen that enters the cathode in air permeates through the membrane to the anode stream. Thus, the nitrogen content at the end of the anode flow stream increases, leading to localized fuel starvation, which can cause carbon corrosion at the cathode electrode.[4] Thus, gas permeability of a PEM and its impact on fuel cell operation is an important parameter that needs to be characterized under different, realistic, fuel cell operating conditions for use in the development and advancement of PEM fuel cells.

Many techniques have been developed to measure the gas permeation rate of the membranes. Among them, in-situ electrochemical measurement of gas permeation is the most direct; where the gas permeation rate is measured as a mass transfer limited current. This article reports on the hydrogen crossover currents measured using the in-situ electrochemical technique. The results are compared to the reported values measured by various techniques. For the known reactant crossover rates, the effects on apparent electrode activity are identified. Also, a mathematical model is developed here to predict the extent of nitrogen accumulation along the anode flow fields, and fuel recycle as a mitigation method is simulated by improving hydrogen distribution. The model results were validated by comparison with experimentally obtained results.

Permeability Coefficient of Proton Exchange Membrane

When different concentrations of hydrogen or oxygen gas exist across a gas permeable membrane, the gases permeate through the membrane due to the partial pressure gradient. The gas pressure applied at each side of the membrane equilibrates to the solubility coefficient (H_i) of the facing side of the membrane, creating the concentration gradient in the membrane. The concentration gradient applied within the membrane drives gas to permeate from one side to the other side of the membrane. The gas permeation rate (N_i) of specie i through a membrane can be expressed as:

$$N_i = D_i \frac{H_i^h p_i^h - H_i^l p_i^l}{l} \qquad (1)$$

Here, if the solubility coefficient is assumed to be a function of temperature and both membrane surfaces are at the same temperature, then the permeability coefficient of specie i can be defined as follows:

$$k_i = D_i H_i = \frac{N_i l}{\Delta p_i} \qquad (2)$$

Therefore, the permeability coefficient can be expressed as the product of the diffusion coefficient and the solubility coefficient. Also, it can be estimated by measuring the permeation rate through the membrane for a given gas pressure difference.

Several measuring techniques have been used to estimate the permeability coefficient of gases in PEMs. These include the volumetric method, time-lag technique, gas chromatography method, and electrochemical monitoring techniques. LaConti et al.[5] and Sakai et al.[2] measured the permeability coefficient of hydrogen and oxygen in Nafion® membranes using the volumetric method. Higher pressure is applied at one side of the membrane and the gas permeation rates are measured at the other side. The time-lag technique is identical to the volumetric method except that the time to fill up fixed volumes downstream of the membrane is measured instead of the flow rate for a given sample area.[6-8] An advantage of this method is that the diffusion coefficient and the solubility coefficient can be broken down from the combined permeability coefficient. Similarly, gas chromatography methods are used by measuring concentration change downstream of the membrane when the same total pressure but different gas concentrations are applied across the membrane.[9]

Another class of measuring the gas permeability coefficient of PEMs is using electrochemical methods. The electrochemical monitoring technique, which monitors current over time for the diffusion limiting condition through the membrane, has been widely used to characterize the gas permeation rates for PEMs.[10-14] In this method, one side of the membrane, which has a working electrode placed at the surface, is exposed to an acid solution with a counter electrode, and current is generated due to the crossover gas, while a reactive gas is supplied to the other side of the membrane and is measured over time to estimate the diffusion coefficient and solubility coefficient of the reactant in the membrane. Also, chronoamperometric techniques with microelectrode or hydrodynamic voltammetry can
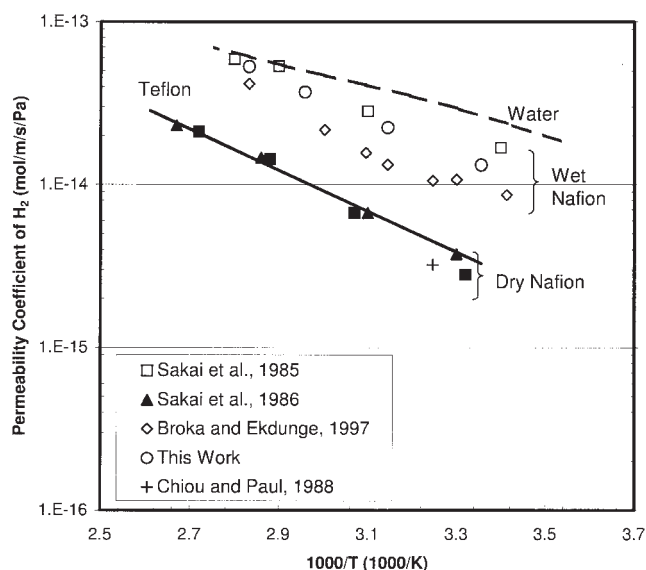
Figure 1. Comparison of hydrogen permeability coefficient of Nafion® 117.

The Nafion® 125 is used for ▲. Lines show the reported hydrogen permeability coefficients of Teflon® and water.

be used to estimate the diffusion coefficient and solubility coefficient.[15-17] However, the chronoamperometric technique and hydrodynamic voltammetry have been used to characterize electrodes by investigating the gas transport rates through the ionomer layer of the electrodes rather than to estimate the gas permeation rate across the membrane because of the microscopic nature of these techniques.

Figures 1 and 2 show the permeation coefficient reported in literature of hydrogen and oxygen of Nafion® membranes. Various measuring techniques are used; however, comparable values are reported. As shown in the figure, a higher permeability coefficient is observed when the membrane was exposed to water approaching values in water,[18,19] while the dried membrane showed a similar or lower values than Teflon®.[20] Sakai et al.[2,6] varied the water content in the membrane by changing the humidity of the gas and demonstrated that the increase of the gas permeability coefficient with higher water content is due to the increase in the diffusion coefficient, while the solubility coefficient of the membrane shows insignificant change. From the results, they claimed that the gas permeates mainly through the water contained ion cluster regions[21] of the membrane.

Ogumi et al.[11,12] investigated hydrogen and oxygen permeation rates for various ion exchange membranes with several ionic forms. Using an estimated ratio of volume fractions between the polymer portion and the water portion in the membrane, insignificant dependency of the volume ratio on the diffusion coefficient is shown for various ionic forms, suggesting that gas permeation is not through the ion cluster region of the membrane. They claimed that the increase in the permeability coefficient with water content is due to the increase of the solubility coefficient in the polymer regions. Based on Yeager's three phase structural model of Nafion®,[22] the intermediate flexible amorphous part of the perfluorocarbon backbone of Nafion® is available for gas dissolution. Since the

volume of the intermediate region can be a significant portion in the membrane when it is hydrated, they concluded that the gases are permeated mainly through the intermediate zone of the membrane by taking advantage of the combination of higher solubility by the Teflon® like properties and a higher diffusion coefficient by the water like properties. Similar conclusions have been drawn from Tsou et al.[13] based on their analysis using Dow's short-side-chain perfluorocarbon membranes.

Figures 1 and 2 also show that the permeability coefficient of gases increases with temperature. Since the membrane water uptake decreases with increasing temperature when vapor water saturated, Broka and Ekdurge[9] show that the highest values of permeability coefficient in the case of hydrated membranes is obtained when the membrane water content is lowest. Founded on this observation, they stated that the mechanism of gas permeation through the membrane involves both hydrated ionic clusters and the intermediate amorphous region of Nafion®. As discussed above, contradicting hypotheses have been suggested to explain the water permeation mechanism through the PEMs due to the complexity of the membrane structure. Further analysis of the mechanisms of permeation for various membrane structures and conditions of the membrane is needed.

In-Situ Electrochemical Technique

As shown in the previous section, gas permeability is a strong function of the membrane conditions, such as hydration level and temperature. Therefore, for operation of PEM fuel cells, the gas permeation rate will vary with change in operation conditions. Even though many methods are available for measuring the gas permeation rate through the proton exchange membranes, in-situ methods to measure the permeation rate are desirable. With an in-situ method, the permeation rate can be
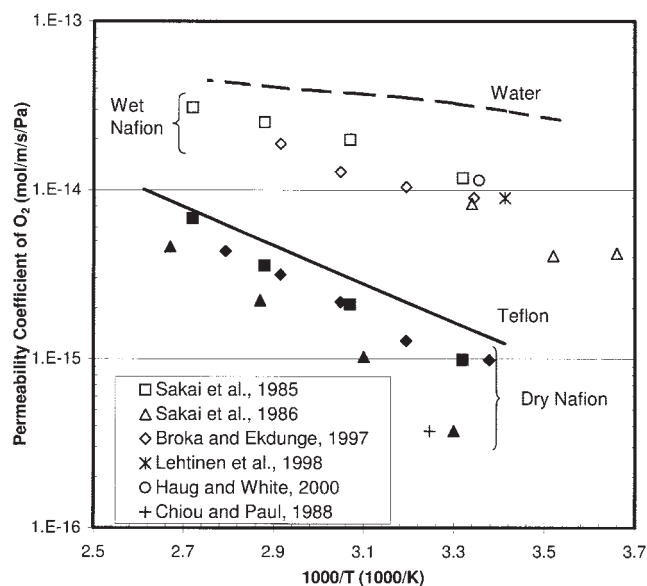

Figure 2. Comparison of oxygen permeability coefficient of Nafion® 117.

The Nafion® 125 is used for ▲ and Δ. Lines show the reported hydrogen permeability coefficients for Teflon® and water.
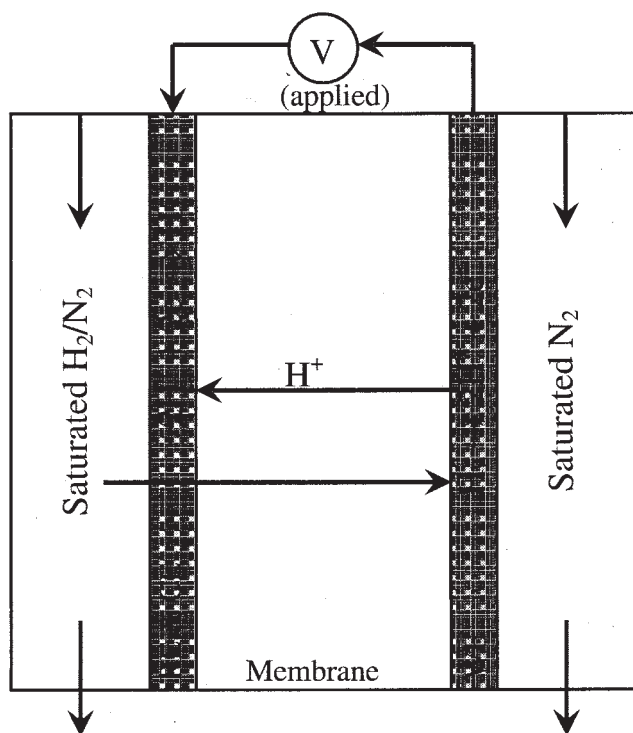
Figure 3. In-situ electrochemical technique for the measurement of the hydrogen permeation rate of a PEM fuel cell (RE—reference electrode, CE—counter electrode, and WE—working electrode).

measured directly in the fuel cell setup; therefore, more realistic values can be obtained without requiring additional test rigs. Also, with the in-situ permeation measuring techniques, gas permeation rates measured before and after endurance runs under load in PEMFC single cells or large stacks can be applied to diagnose membrane degradation over time.

Figure 3 shows the experimental conditions from the fuel cell setup for in-situ measuring of the gas permeation rate. Hydrogen flows on one side of a fuel cell and the electrode of this side function as the reference and counter electrode. The reactant crosses over to the other side of the membrane and gets oxidized at the other electrode (working electrode) by the application of a voltage, and the resulting current is measured. The current generated in this configuration reaches limiting values within a few hundred mille volts. Thus, the crossover current density of reactant i, $i_{i,x}$, is defined as the current generated for the permeated reactant through the membrane, and the gas permeation coefficient of the membrane can be expressed as:

$$k_i = \frac{i_{i,x}}{nF} \frac{l}{p_i} \qquad (3)$$

The experiments were carried out in the 26 cm^2 active area fuel cell setup using a UTC Fuel Cells' water management design.[23,24] Humidified 4% hydrogen remaining nitrogen was flown on the anode side, and the cathode was exposed to humidify nitrogen. The anode served as the reference electrode

as well as counter electrode, and the cathode is the working electrode. A PAR 273 potentiostat (EG&G) was used to scan or apply voltages to measure the resulting crossover currents. Typically, a scan rate of 0.1 mV/s or lower was employed to obtain limiting crossover currents.

Typical crossover currents are depicted in Figure 4 for a Nafion® 112 membrane at 65°C with saturated hydrogen at 100 kPa total pressure. As the applied voltage increases, the crossovered hydrogen consumption rate at the cathode electrode increases, showing a rapid increase in current density. Then, it plateaus starting around ~0.1 volt as the current is now limited by the hydrogen permeation rate of the membrane. This crossover current density ($i_{H2,x}$) is linearly proportional to the feed partial pressure of the reactant (p_i) and the permeability coefficient of the membrane (k_{H2}) and inversely proportional to the thickness of the membrane (l) as it is described in Eq. 3.

Figure 5 shows a case showing linearly increasing current superimposed in the limiting current region. This is an indication of an electrical short in the membrane and electrode assembly (MEA), the magnitude of which is equal to the inverse of the slope (V/I). When there is no significant electrical short in the fuel cells, the crossover current (I_x) should be equal to the measured current (I_L). With a short current, I_L becomes higher due to the current flows through the electrical short (I_s). The electrical short current linearly increases with the applied voltage (V_{cell}) and is inversely proportional to the resistance of the short (R_s). Therefore, the following correlation is used to estimate a corrected crossover current density.

$$i_x = \frac{I_L}{A} - \frac{V_{cell}}{R_s A} \qquad (4)$$

Figure 5 also shows the simulated current responses for various magnitudes of electrical shorts (R_s). This illustrates that this cell has about 1.9 ohm electrical short. The technique has been used as a diagnostic tool to quantitatively separate the
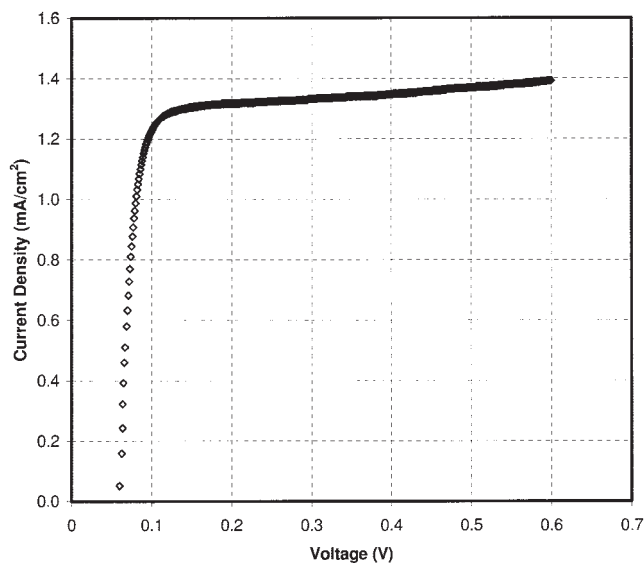

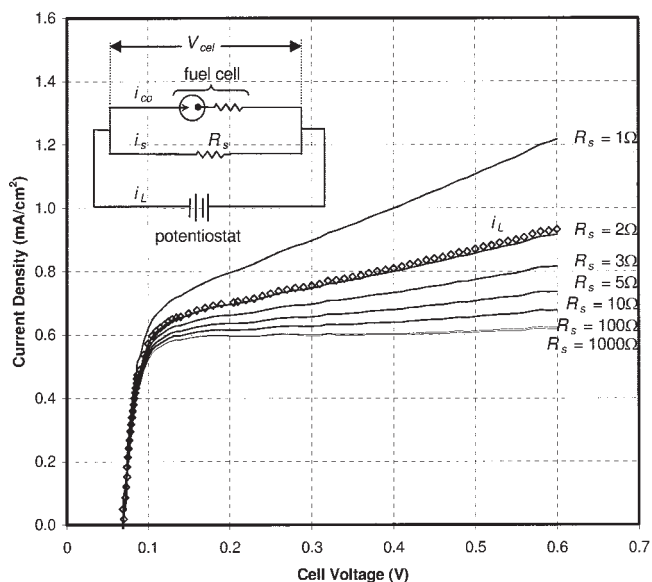**Figure 4. A typical case for the measurement of the crossover current density.**

Figure 5. Effect of electrical short in the membrane and electrode assembly on the measurement of the gas crossover current density.

Figure 7. In-situ hydrogen crossover currents vs. hydrogen partial pressure in Nafion® 111 membrane.

effects of crossover from electrical shorting, both of which lower the open circuit voltage as well as the cell voltage.[25]

Figure 6 shows hydrogen crossover currents measured for Nafion® 112 over a range of temperatures and pressures in a fuel cell under saturated gases. The crossover currents were measured at 0.4 V over a period of 15 minutes to obtain steady-state values at each temperature and pressure. Linearly increasing crossover current is shown as it is expected in Eq. 3, and higher crossover current density is observed for higher temperature. A 25 μm thick membrane was also tested, and the results are shown in Figure 7. Higher crossover current densi-
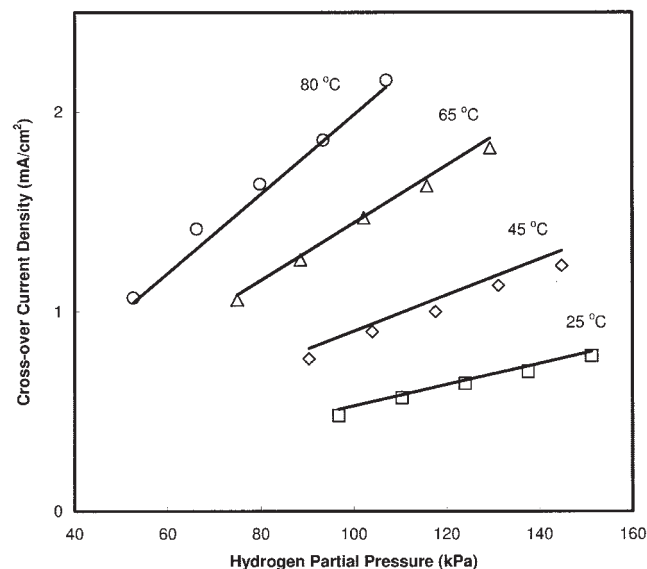
ties are measured with this thinner membrane due to the decrease in the permeation distance through the membrane as it is described in Eq. 3. The same trends for pressure and temperature are shown with this membrane.

From the results shown in Figures 6 and 7, the hydrogen permeability coefficient of the Nafion® membrane is estimated for various thickness and hydrogen partial pressure as shown in Figure 8. The results of this analysis are summarized in Eq. 5. The activation energy for hydrogen permeation ($E_{p,H2}$) is estimated to be 21.03 kJ/mol for the Nafion® membrane used in the experiments at the fuel cell conditions.

$$k_{H2} = 6.6 \times 10^{-11} \exp\left(-\frac{21.03 \text{ kJ/mol}}{RT}\right) \qquad (5)$$

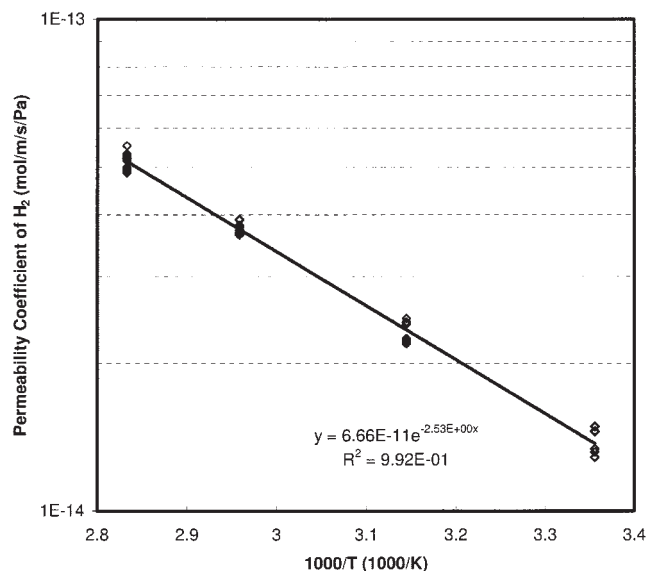**Figure 6. In-situ hydrogen crossover currents versus hydrogen partial pressure in Nafion® 112 membrane.**
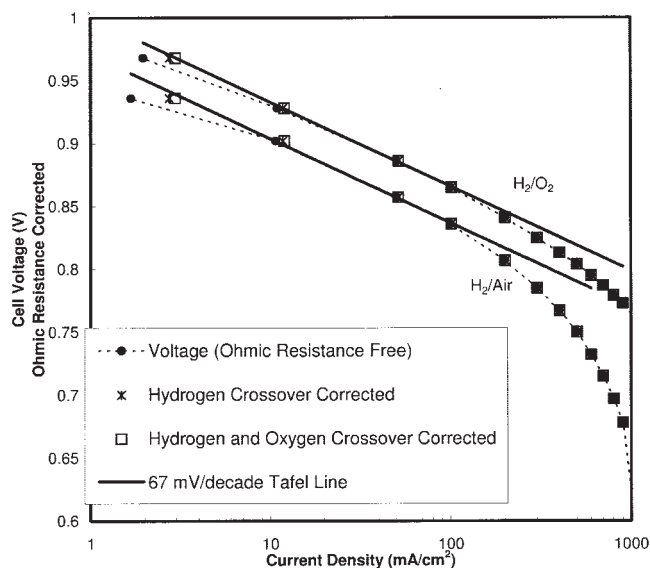

Figure 8. Hydrogen permeability coefficient of Nafion®.

Figure 9. Effect of reactant crossover on cell performance at T = 65°C and near-ambient pressure.

The estimated values of the hydrogen permeability coefficient are compared to the values shown in Figure 1. The values are matched well for the wet membranes.

Activity Measurement with Reactant Crossover Corrections

In operating fuel cells, the hydrogen permeated across the membrane from anode to the cathode, is oxidized at the cathode electrode. It could be chemically oxidized due to the presence of hydrogen and oxygen on platinum, or it could be electrochemically oxidized with high over-potential of hydrogen reaction at the cathode. Assuming electrochemical oxidation only, the protons and electrons produced from this crossover hydrogen electrochemical oxidation will be consumed without generating an external current. The effect of the crossovered hydrogen is more significant at lower current densities, affecting the apparent activity of the electrochemical reactions. Figure 9 shows the effects of reactant crossover on polarization curves for a cell made using a Nafion® 112 membrane. The hydrogen permeability reported previously is used, and half of the hydrogen permeability is used for oxygen permeation after correcting for concentration of oxygen at ambient air.[2] The correction of the crossover is mainly noticeable at very low current densities. After the correction, the polarization plots showed better linear correlation to the theoretical Tafel lines at the lower current densities. This supports the assumption that the crossovered reactants are consumed electrochemically. With this crossover correction, the activity of the catalyst can be more accurately assessed.

Effect of Gas Crossover on a Hydrogen Delivery System

When inert gases flow through the cells, the gases also permeate across the membrane. For a pure hydrogen-air system, nitrogen and oxygen gas permeate through the membrane

to the anode side while hydrogen permeates from the anode to the cathode. Hydrogen and oxygen crossover through the membrane are consumed without generating useful energy, as discussed before. On the other hand, nitrogen crossover through the membrane accumulates at the end of the anode flow fields, leading to local fuel starvation. It has been reported that this local fuel starvation leads to cathode catalyst degradation.[4] Thus, a means to eliminate local starvation of hydrogen is necessary for long-life fuel cells. Here, we report the effect of nitrogen crossover to the anode stream by modeling the fuel delivery system with fuel recycle as a means to eliminate local fuel starvation.[26] A one-dimensional steady-state model along the anode stream is developed. The isothermal assumption is used. With this model, the nitrogen distribution is calculated and the modeling results of the nitrogen exit concentration are then compared with experimental results.

The modeling domain is shown in Figure 10. On the anode side, hydrogen enters at the inlet $x = 0$. As the gas moves down along the channel, the hydrogen content decreases due to electrochemical reaction to generate useful electricity and undesirable losses as a result of hydrogen crossover and oxygen crossover. While the hydrogen content is decreasing, the nitrogen content increases due to nitrogen crossover from the cathode side. A mass balance on a control volume in the anode side yields the following differential equation for the anode stream:

$$\frac{dN_i}{dX} + \frac{L(w_c + w_r)}{h_c w_c} n_i = 0 \tag{6}$$
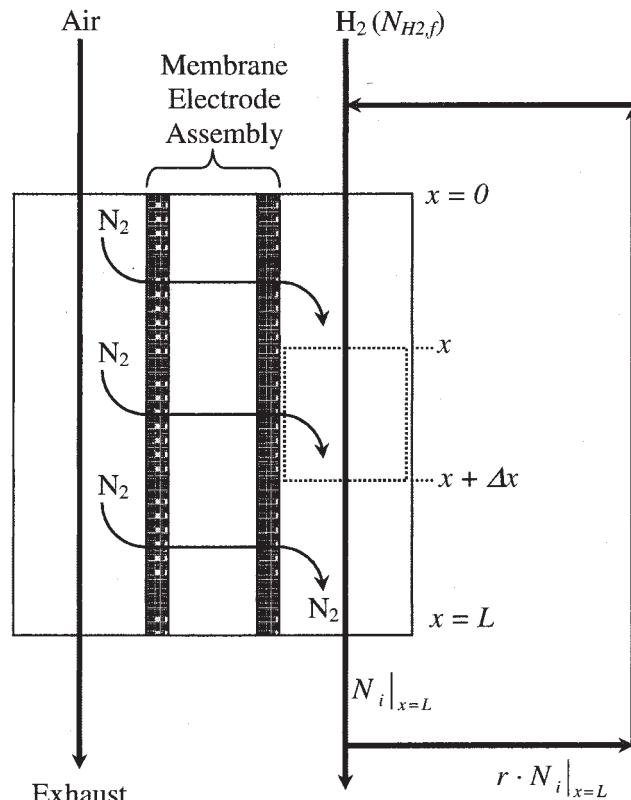

Figure 10. Model domain and experimental setup.

Hydrogen and oxygen crossover are not shown.

where the consumption rate of hydrogen and nitrogen in a anode stream are shown below:

$$n_{H2} = \frac{i_e}{2F} + \frac{k_{H2}}{l}\left(\frac{N_{H2}}{N_{H2} + N_{N2}}\right)p^a + \frac{k_{O2}p_{O2}^c}{2l} \qquad (7)$$

$$n_{N2} = -\frac{k_{N2}}{l}\left(p_{N2}^c - \frac{N_{N2}}{N_{H2} + N_{N2}}p^a\right) \qquad (8)$$

Equation 7 describes the consumption of hydrogen due to electrochemical reaction, hydrogen losses due to its crossover to the cathode side, and its consumption due to the permeation of oxygen from the cathode side. For simplicity, uniform current distribution along the gas stream is assumed. Also, the permeated hydrogen and oxygen is reacted instantaneously. For the present configuration, the flow field pressure drop is small, and thus the total pressure, p^a, is assumed constant. Eq. 8 describes the nitrogen crossover from the cathode to the anode due to concentration gradients. Here, constant nitrogen concentration in the cathode side is assumed.

The flux of hydrogen and nitrogen in the anode stream along the channel is obtained by combining the above equations, and is shown below:

$$\frac{w_c h_c}{L(w_c + w_r)}\frac{dN_i}{dX} = -\alpha_i\left(\frac{N_i}{N_{H2} + N_{N2}}\right) + \beta_i \qquad (9)$$

where:

$$\alpha_{H2} = \frac{k_{H2}p^a}{t}, \text{ and } \alpha_{N2} = \frac{k_{N2}p^a}{t} \qquad (10)$$

$$\beta_{H2} = -\left(\frac{i_e}{nF} + \frac{k_{O2}p_{O2}^c}{2t}\right), \text{ and } \beta_{N2} = \frac{k_{N2}p_{N2}^c}{t} \qquad (11)$$

At the anode inlet, the gas concentration is fixed by the feed concentration and the gas recycle rate shown by Eq. 12. The feed concentration can be described as functions of the applied current density (i_e) and the electrochemical hydrogen utilization (U_e) as described by Eq. 13. The calculated exit concentration of gases is used to set the inlet concentration when the stream is recycled. Here, the recycle rate, r, is defined as the ratio of gas recycled over the exit gas flow rate.

$$N_{i,o} = N_{i,f} + rN_i|_{X=1} \qquad (12)$$

$$N_{H2,f} = \frac{i_e}{nFU_e}\frac{(w_r + w_c)L}{w_c h_c} \qquad (13)$$

The gas concentration as a function of position is calculated by Microsoft Excel software applying the fourth-order Runge Kutta method. Once the molar flux rates of hydrogen and nitrogen are calculated along the anode stream, the mole fraction of nitrogen can be expressed as:

$$y_{N2}(X) = \frac{N_{N2}}{N_{N2} + N_{H2}} \qquad (14)$$
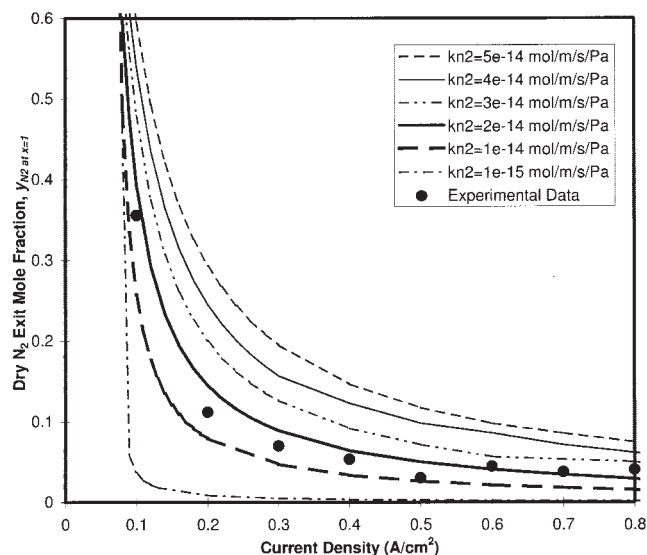

Figure 11. Comparison of experimental and simulated results on the anode exit nitrogen content for various current densities.

$U_e = 0.95$, $r = 0$, ambient pressure = 338K.

In this calculation, the hydrogen crossover rate is computed with the experimental results described in a previous section. The oxygen crossover rate is assumed to be half of the hydrogen crossover rate.[2]

To estimate the nitrogen crossover rate, the gas concentration at the exit of the anode stream is measured, and compared to the model. The experimental setup shown in Figure 10 is used. A UTC Fuel Cells inter-water management cell design with 400 cm^2 active area is used for the experiments. A gas sampling port was installed at the fuel exit location. A small sample stream of the total gas stream is continuously analyzed with gas chromatography. Then, the nitrogen concentration of the exit stream is measured for various current densities when the hydrogen stream is fed at 95% of U_e with no recycle. Figure 11 shows the experimental results compared to model estimations at various nitrogen permeability coefficient values. From this comparison, the nitrogen permeability coefficient of the membrane is estimated to be 1.5×10^{-14} mol/m/s/Pa. Since a UTC Fuel Cells water transport plate (WTP) design is used for this experiment, it is reasonable to assume that the membrane is directly contacted to liquid water during operation. As shown in Figures 1 and 2, the permeability coefficient of wetted Nafion® is expected to be higher than the dry permeability coefficient in Teflon® and closer to the permeability coefficient in water. In Figure 12, the estimated permeability coefficient of nitrogen is compared to the values in water and Teflon. Also, the nitrogen permeability coefficients of a dry Nafion® membrane reported by Chiou and Paul[8] are plotted. As expected, the permeability coefficient of nitrogen from this experiment was higher than the value of the dry Nafion® membrane as well as the Teflon but lower than the value for liquid water. This provides confidence in our estimations and basis of further analysis of the model results.

Figure 11 shows that the exit nitrogen concentration increases exponentially as the current density decreases. This is because the nitrogen crossover rate increasingly becomes a
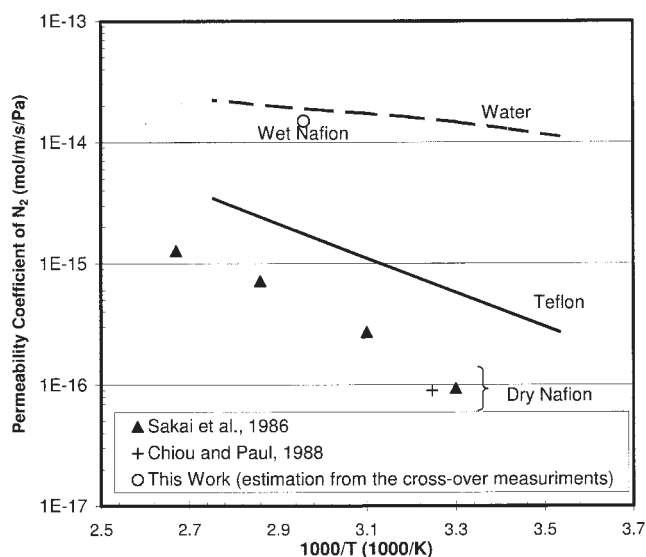
Figure 12. Comparison of nitrogen permeability coefficient of Nafion® to water and Teflon®.

Figure 13. Effect of electrochemical hydrogen utilization on the total hydrogen utilization at various current densities.

larger portion of the total exit flow rate as the current density decreases while U_e is fixed. At a fixed U_e of the anode side, the inlet hydrogen flow rate is fixed for a given current density. This concentration of hydrogen decreases along the flow channel due to consumption while the nitrogen concentration increases due to crossover from the cathode. This effect is more significant at lower current densities because the hydrogen flow rate is lower at lower current density while the crossover rates are essentially constant. This phenomenon can be explained by introducing the concept of the total reactant utilization (U_t) shown in Eq. 15. The U_t is the ratio of the total consumption rate of hydrogen to that of the total inlet flow. The total consumption includes useful electrochemical reaction and consumption due to crossover through the membrane. As shown in Figure 13, at a fixed U_e, the U_t rapidly increases as the current density decreases. For an example, for a reactant flow fixed at 95% of U_e, the U_t increases to 95.5% at 0.6 A/cm² due to the effect of gas crossover, and it increases to 98% as the current density decreases to 0.1 A/cm²:

$$U_t = U_e + \frac{(w_r + w_c)}{N_{H2,i} w_c h_c} \left(\frac{k_{O2} p_{O2}^c L}{2t} + \int_0^1 \frac{k_{H2}}{t} \left(\frac{N_{H2}}{N_{H2} + N_{N2}} \right) p^a dX \right) \quad (15)$$

The nitrogen concentration profile as a function of position is simulated and is shown in Figure 14. At the inlet location, the nitrogen concentration is zero; as we move downstream, the concentration increases. The accumulation of nitrogen is more significant at lower current densities, as discussed before. Interestingly, the nitrogen accumulates to an appreciable amount only at the last 5 to 10% of the total length of the channel. This is a potential fuel starvation situation and may lead to cathode carbon corrosion. This local nitrogen buildup can be minimized
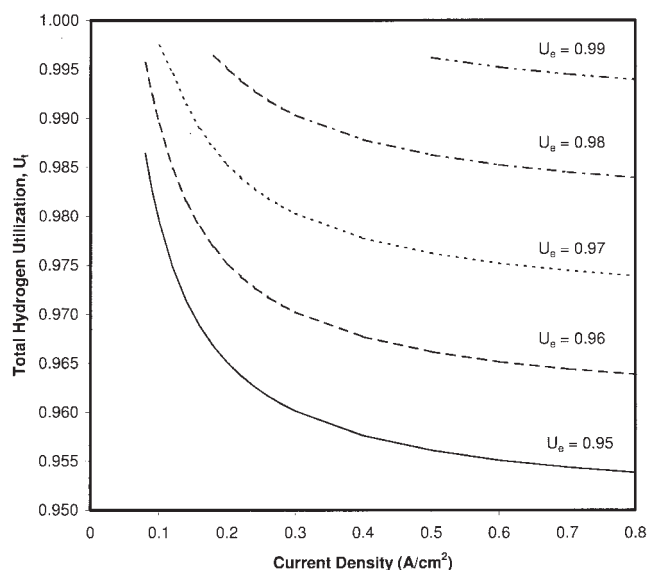
with a fuel recycle.[26] A recycle blower may be used to circulate the fuel. As shown in Figure 15, the nitrogen composition is becoming more uniform as the recycle rate increases. With an increase in the recycle ratio, the inlet nitrogen concentration increases from the contribution of the recycled nitrogen. Thus, the total nitrogen content in the anode stream increases as the recycle ratio increases. However, this decreases the driving force for nitrogen crossover. Thus, the exit nitrogen concentration is reduced. This could be a critical consideration to develop a high fuel utilization fuel cell system to meet the hydrogen emission safety standards, minimizing the possibility of carbon corrosion performance decay.
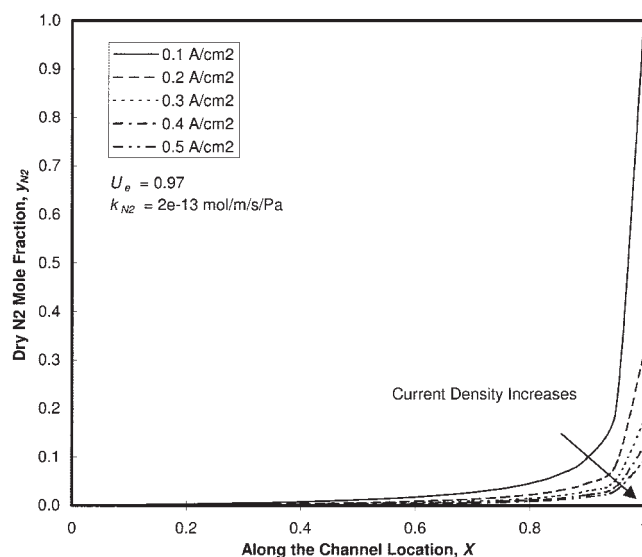

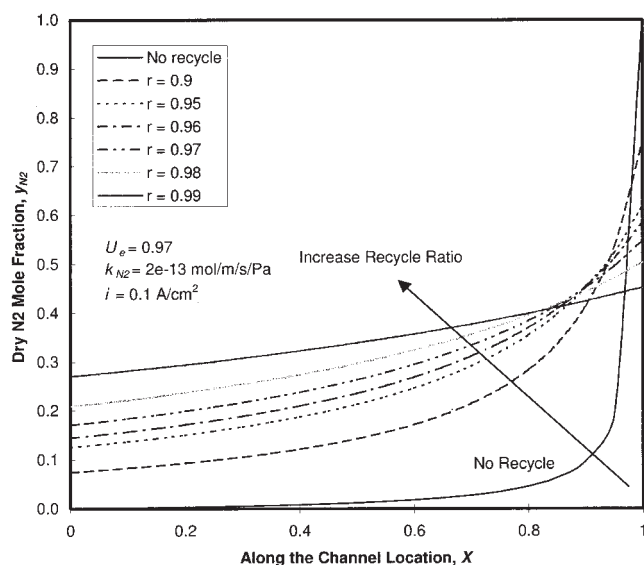**Figure 14. Simulated nitrogen profile as a function of position.**

Figure 15. Effect of fuel recycles on the distribution of nitrogen in the anode stream.

Conclusions

The permeability and permeation rates of hydrogen in proton exchange membranes can be determined using an in-situ electrochemical technique at various temperatures, pressures, and humidities. The hydrogen permeability coefficients of a Nafion® membrane estimated in this study are in agreement with values obtained by traditional techniques reported in the literature. The measurements may be used as diagnostic tools to determine increased crossover or presence of an electrical short in the membrane electrode assembly. Also, the crossover correction allows a better estimation of catalyst activity in a fuel cell.

A mathematical model is developed to predict the nitrogen content of an anode with high fuel utilization. The nitrogen permeability coefficient through the membrane has been estimated by comparing the experimental results with mathematical model analysis. Simulation indicates that a considerable amount of nitrogen builds up at the last 5 to 10% of the exit location. Anode fuel recycle is recommended as a remedy of a potential local fuel starvation situation.

Acknowledgments

Notation

A = active area, m^2
D = effective diffusion coefficient, m^2/s
E = activation energy of gas permeation through membrane, J/mol
F = Faraday's constant, 96,487 C/equiv
H = solubility coefficient, $mol/m^3/Pa$
h = height of channel, m
i = current density, A/m^2
I = current, A
k = permeability coefficient, mol/m/s/Pa
l = thickness of membrane, m
L = length of flow channel, m
n = number of electrons

n_i = molar consumption rate of specie i, $mol/m^2/s$
N = molar flux of specie i, $mol/m^2/s$
p = pressure, Pa
p_i = partial pressure of specie i, Pa
R_s = electrical resistance of short, Ω
R = gas constance, 8.314 J/mol/K
r = recycle ratio
T = Temperature, K
U = reactant utilization
w = width, m
x = distance of channel, m
X = dimensionless position along the anode channel (x/L)
y = mole fraction of gas

Greek letters

α = dimensionless constant defined in Eq. 11
β = dimensionless constant defined in Eq. 10

Indices

a = anode
c = cathode
c = channel
$cell$ = cell
e = electrochemical
f = feed
$H2$ = hydrogen
h = high side
i = specie (H_2, N_2, or O_2)
L = through the potentiostat
l = low side
o = inlet
$O2$ = oxygen
t = total
r = rib of flow field
x = crossover

Literature Cited

1. St-Pierre J, Wilkinson DP. Fuel cells: a new, efficient and cleaner power source. *AIChE J.* 2001;47:1482–1486.
2. Sakai T, Takenaka H, Wakabayashi N, Kawami Y, Torikai E. Gas permeation properties of solid polymer electrolyte (SPE) membranes. *J Electrochem Soc.* 1985;132:1328–1382.
3. LaConti AB, Hamdan M, McDonald RC. Mechanisms of membrane degradation. In: Vielstich W, Gasteiger HA, Lamm A. *Handbook of Fuel Cells—Fundamentals, Technology and Applications, Volume 3: Fuel Cell Technology and Applications*. Chichester, UK: Wiley; 2003.
4. Reiser CA, Bregoli L, Patterson TW, Yi JS, Yang JD, Perry ML, Jarvi TD. A reverse-current decay mechanism for fuel cells. *J Electrochem Solid-State Letters.* 2005;8:A273–A276.
5. LaConti AB, Fragala AR, Boyack JR. Solid polymer electrolyte electrochemical cells: electrode and other materials considerations. In: McIntyre JDE, Srinivasan S, Will FG. *Electrode Materials and Processes for Energy Conversion and Storage*. Pennington, NJ: The Electrochemical Society, Inc., 1977;PV77–6:354–374.
6. Sakai T, Takenaka H, Torikai E. Gas diffusion in the dried and hydrated Nafions. *J Electrochem Soc.* 1986;133:88–92.
7. Sakai T, Takenaka H, Torikai E. Oxygen/nitrogen separation by a Nafion®-Ag microcomposite membrane. *J Membr Sci.* 1987;31:227–234.
8. Chiou JS, Paul DR. Gas permeation in a dry Nafion membrane. *Ind Eng Chem Res.* 1988;27:2161–2164.
9. Broka K, Ekdunge P. Oxygen and hydrogen permeation properties and water uptake of Nafion® 117 membrane and recast film for PEM fuel cell. *J Appl Electrochem.* 1997;27:117–123.
10. Yeo RS, McBreen J. Transport properties of Nafion membranes in electrochemically regenerative hydrogen/halogen cells. *J Electrochem Soc.* 1979;126:1682–1687.
11. Ogumi Z, Takehara Z, Yoshizawa S. Gas permeation in SPE method I. Oxygen permeation Through Nafion and NEOSEPTA. *J Electrochem Soc.* 1984;131:769–773.

12. Ogumi Z, Kuroe T, Takehara Z. Gas permeation in SPE method II. Oxygen and hydrogen permeation through Nafion. *J Electrochem Soc.* 1985;132:2601–2605.

13. Tsou Y, Kimble MC, White RE. Hydrogen diffusion, solubility, and water uptake in Dow's short-side chain perfluorocarbon membranes. *J Electrochem Soc.* 1992;139:1913–1917.

14. Haug AT, White RE. Oxygen diffusion coefficient and solubility in a new proton exchange membrane. *J Electrochem Soc.* 2000;147:980–983.

15. Lawson DR, Whiteley LD, Martin CR, Szentirmay MN, Song JI. Oxygen reduction at Nafion film-coated platinum electrodes: transport and kinetics. *J Electrochem Soc.* 1988;135:2247–2253.

16. Parthasarathy A, Martin CR, Srinivasan S. Investigations of the oxygen reduction at platinum/Nafion® interface using a solid-state electrochemical cell. *J Electrochem Soc.* 1991;138:916–921.

17. Watanabe M, Igarashi H, Yosioka K. An experimental prediction of the preparation condition of Nafion-coated catalyst layers for PEFCs. *Electrochim Acta.* 1995;40:329–334.

18. Sander R. *Compilation of Henry's Law Constants for Inorganic and Organic Species of Potential Importance in Environmental Chemistry (Version 3).* Mainz, Germany: Max-Planck Institute of Chemistry; 1999.

19. Reid RC, Prausnitz JM, Poling BE. *The Properties of Gases & Liquids (4th ed).* Boston: McGraw-Hill; 1987.

20. Pasternak RA, Christensen MV, Heller J. Diffusion and permeation of oxygen, nitrogen, carbon dioxide, and nitrogen dioxide through polytetrafluoroethylene. *Macromolecules.* 1970;3:366–371.

21. Gierke TD, Munn GE, Wilson FC. The morphology in Nafion perfluorinated membrane products, as determined by wild- and small-angle X-ray studies. *J Polym Sci.* 1981;19:1687–1904.

22. Yeager HL, Steck A. Cation and water diffusion in Nafion ion exchange membranes: influence of polymer structure. *J Electrochem Soc.* 1981;128:1880–1884.

23. Reiser CA. Ion exchange membrane fuel cell power plant with water management pressure differentials. *US Patent 5,*700,595; 1997.

24. Yi JS, Yang JD, King C. Water management along the flow channels of PEM fuel cells. *AIChE J.* 2004;50:2594–2603.

25. Kocha SS. Principles of MEA preparation. In: Vielstich W, Gasteiger HA, Lamm A. *Handbook of Fuel Cells—Fundamentals, Technology and Applications. Volume 3: Fuel Cell Technology and Applications.* Chichester, UK: Wiley; 2003.

26. Reiser CA. High fuel utilization in a fuel cell. *US Patent 6,*558,827 B1; 2003.